



Title	Exploring enzymatic degradation, reinforcement, recycling, and upcycling of poly(ester)-poly(urethane) with movable crosslinks
Author(s)	Liu, Jiaxiong; Ikura, Ryohei; Yamaoka, Kenji et al.
Citation	Chem. 2025, 11(2), p. 102327
Version Type	VoR
URL	<a href="https://hdl.handle.net/11094/100602">https://hdl.handle.net/11094/100602</a>
rights	This article is licensed under a Creative Commons Attribution 4.0 International License.
Note	

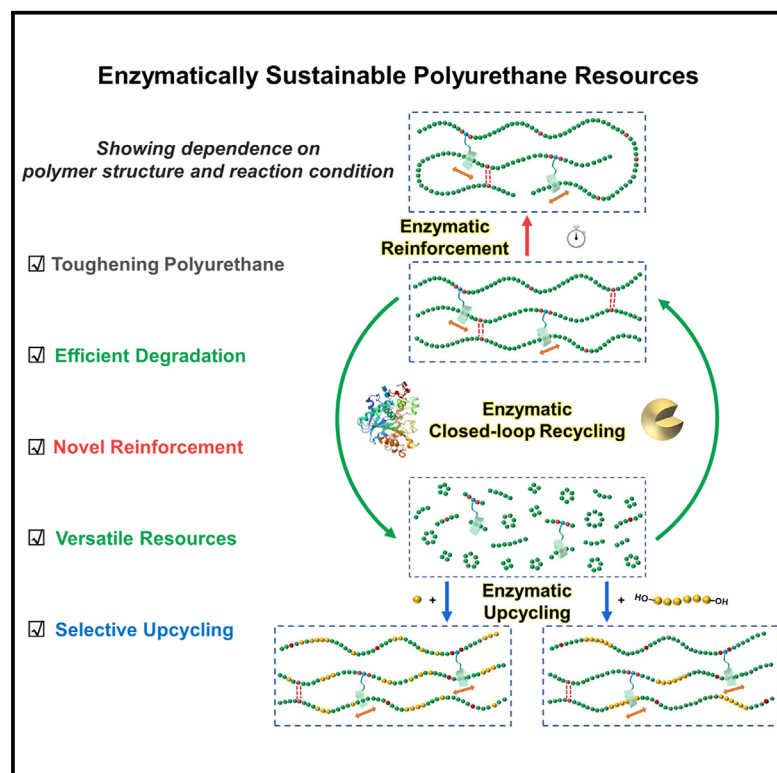
*The University of Osaka Institutional Knowledge Archive : OUKA*

<https://ir.library.osaka-u.ac.jp/>

The University of Osaka

# Exploring enzymatic degradation, reinforcement, recycling, and upcycling of poly(ester)-poly(urethane) with movable crosslinks

## Graphical abstract



## Highlights

- Introducing cyclodextrin-based movable crosslinks toughens polyurethane
- Enzymatic degradation of polyurethane is optimized due to the bulky cyclodextrin
- Novel enzymatic reinforcement strategy to enhance polyurethane mechanical properties
- Enzymatic closed-loop recycling and selective upcycling

## Authors

Jiaxiong Liu, Ryohei Ikura, Kenji Yamaoka, ..., Junsu Park, Hiroshi Uyama, Yoshinori Takashima

## Correspondence

uyama@chem.eng.osaka-u.ac.jp (H.U.), takasima@chem.sci.osaka-u.ac.jp (Y.T.)

## In brief

A facile polymer structure design combined with enzymatic reaction was developed to achieve tough and sustainable polyurethane (PU) resources. Introducing cyclodextrin-based movable crosslinks toughened the poly( $\epsilon$ -caprolactone)-poly(urethane) (PCL-PUs) and optimized the enzymatic degradation efficiency. Under reaction time control, molecular weight and mechanical properties of PCL-PUs with movable crosslinks were enhanced by a novel enzymatic reinforcement strategy. The prepared polymers can be enzymatically closed-loop recycled by switching the reaction concentration or upcycled into value-added polymers with selective substrates.



Liu et al., 2025, Chem 11, 102327  
February 13, 2025 © 2024 The Author(s).  
Published by Elsevier Inc.  
<https://doi.org/10.1016/j.chempr.2024.09.026>

## Article

# Exploring enzymatic degradation, reinforcement, recycling, and upcycling of poly(ester)-poly(urethane) with movable crosslinks

Jiaxiong Liu,<sup>1</sup> Ryohei Ikura,<sup>1,3</sup> Kenji Yamaoka,<sup>1,3</sup> Akihide Sugawara,<sup>2</sup> Yuya Takahashi,<sup>5</sup> Bunsho Kure,<sup>5</sup> Naomi Takenaka,<sup>5</sup> Junsu Park,<sup>1,3</sup> Hiroshi Uyama,<sup>2,\*</sup> and Yoshinori Takashima<sup>1,3,4,6,\*</sup>

<sup>1</sup>Department of Macromolecular Science, Graduate School of Science, Osaka University, 1-1 Machikaneyama, Toyonaka 560-0043, Osaka, Japan

<sup>2</sup>Division of Applied Chemistry, Graduate School of Engineering, Osaka University, 2-1 Yamadaoka, Suita 565-0871, Osaka, Japan

<sup>3</sup>Forefront Research Center, Graduate School of Science, Osaka University, 1-1 Machikaneyama, Toyonaka 560-0043, Osaka, Japan

<sup>4</sup>Innovative Catalysis Science Division, Institute for Open and Transdisciplinary Research Initiatives (ICS-OTRI), Osaka University, 1-1 Yamadaoka, Suita 565-0871, Osaka, Japan

<sup>5</sup>Nara Laboratory, Kyoeisha Chemical Co., Ltd., 5-2-5 Saikujō, Nara 630-8453, Japan

<sup>6</sup>Lead contact

\*Correspondence: [uyama@chem.eng.osaka-u.ac.jp](mailto:uyama@chem.eng.osaka-u.ac.jp) (H.U.), [takashima@chem.sci.osaka-u.ac.jp](mailto:takashima@chem.sci.osaka-u.ac.jp) (Y.T.)

<https://doi.org/10.1016/j.chempr.2024.09.026>

**THE BIGGER PICTURE** Developing tough and sustainable polymer resources, such as polyurethane (PU), is an effective method to address the issue of polymeric materials waste. Enzymes are highly efficient and sustainable biocatalysts, emerging as an ecological technology to advance the circular plastics economy. However, enzymatic degradation is restricted by crystallization in solids or aggregation in the solution of polymeric materials.

Herein, we introduced bulky cyclodextrin-based movable crosslinks to toughen PU and facilitate the enzymatic degradation toward more sustainable PU resources. Under selective reaction conditions, enzymatic degradation, reinforcement, recycling, and upcycling of PU with movable crosslinks were successfully performed, highlighting the significance of polymer structure and reaction condition design. The innovative combination of polymer structure design and enzymatic reaction has the potential to be applied to diverse polymer resources, thereby contributing to a sustainable world.

## SUMMARY

Enzymes are highly efficient, chemoselective, and sustainable biocatalysts, standing out as eco-friendly tools to advance the circular plastics economy. Herein, we explored enzymatic reactions of poly( $\epsilon$ -caprolactone)-poly(urethane) (PCL-PUs) in organic solvent under different reaction conditions using Novozym 435 (immobilized lipase) as the enzyme. PCL-PUs with triacetylated  $\gamma$ -cyclodextrin (TAc $\gamma$ CD)-based movable crosslinks (PCL- $\gamma$ CD-PU) not only exhibited excellent mechanical properties due to effective energy dissipation, but also efficient enzymatic degradation that was optimized for increases in TAc $\gamma$ CD content. Under reaction time control, molecular weight and mechanical properties of PCL- $\gamma$ CD-PU were enhanced by a novel enzymatic reinforcement strategy. Without sorting, the degraded products are versatile resources that can be enzymatically closed-loop recycled by switching reaction concentration or enzymatically upcycled into value-added polymers by mixing with selective substrates. The facile polymer structure design combined with enzymatic reactions is expected to provide a broad approach for toughening various polymeric materials and advancing their development as sustainable resources.

## INTRODUCTION

Tough polymeric materials play a significant role in modern development, while their end-of-life waste has become an urgent environmental issue.<sup>1–3</sup> Instead of focusing solely on solv-

ing the polymeric materials waste disposal problem, advancing polymeric materials, such as polyurethane (PU), to function as sustainable resources would be more effective and eco-friendly.<sup>4–6</sup> Owing to the easy and tunable polyaddition of a diol (or polyol) onto a diisocyanate to form stable urethane



linkages, PU has remarkable chemical diversity and durability, which make it applicable in many areas, such as foams, adhesives, coats, and elastomers.<sup>7,8</sup> However, these beneficial properties of PU also limit the opportunity for energy-efficient degradation and recycling.<sup>9,10</sup> As a result, most end-of-life PU is still landfilled or incinerated, leading to waste disposal problem. The developed method that focuses on urethane linkages is promising, while the low reactivity under mild conditions hinders development.<sup>9–11</sup> Alternatively, the introduction of polyols (e.g., polycaprolactone and polylactide) with readily cleavable bonds, through which PU can be easily broken down and recomposited as circular polymer resources, is broad, sustainable, and energy-saving.<sup>10,12–19</sup>

Numerous catalysts have been developed to solve the issue mentioned above.<sup>20–22</sup> Compared with chemical processes, enzymes are highly efficient, chemoselective, and sustainable biocatalysts that have been developed in academia and industry, standing out as environmentally benign technology.<sup>23–27</sup> With a broad range of substrates and reaction types, enzymes hold great potential for advancing the development of various polymeric materials with complex chemical compositions and structures into sustainable resources.<sup>25–27</sup> In addition, enzymes exhibit a powerful ability to selectively attack specific groups while leaving the others intact under mild conditions, affording the opportunity to deconstruct complex PU into specific building blocks for recycling or upcycling.<sup>27–30</sup> Lipase-catalyzed degradation of poly(urethane-ester) in organic solvent produced ester-breakage products,<sup>31</sup> which can potentially be recycled or further upcycled using the same lipase.<sup>32–34</sup>

However, crystallization in solid or chain aggregation in solution of polymeric materials hinders the access of polymer substrates to enzymes, thus resulting in relatively low enzymatic efficiency.<sup>35–39</sup> Paradoxically, to meet modern demands, strong interactions or aggregation between polymer chains are needed to maintain the mechanical properties of polymeric materials.<sup>40–44</sup> Without adequate mechanical properties, the practicality and applications of polymeric materials would be severely limited. To this end, a facile approach to polymer structure design is needed to balance the contradiction. Previously, we successfully weakened the chain interactions and improved the mechanical properties of PU by introducing bulky cyclodextrin (CD)-based movable crosslinks,<sup>45</sup> which may facilitate enzymatic reactions of polymeric materials. Moreover, CDs are commercially available, nontoxic, and biodegradable and have been widely developed, ranging from polymeric materials to biomedicine.<sup>46–53</sup> Thus, CD-based movable crosslinks combined with enzymatic reactions may contribute to designing tough and sustainable PU resources to enhance their circular economy.

Herein, we prepared poly( $\epsilon$ -caprolactone)-poly(urethane) (PCL-PU) with different structures and studied their reactions catalyzed by Novozym 435 as the enzyme in organic solvent. PCL-PU with triacetylated  $\gamma$ -CD (TAC $\gamma$ CD)-based movable crosslinks (PCL- $\gamma$ CD-PU) exhibited excellent mechanical properties and enzymatic degradation efficiency. Further investigation demonstrated that the enzymatic reaction behaviors of PCL- $\gamma$ CD-PU can be regulated by reaction conditions, including

enzyme contents, reaction time, concentration, and substrate structures. Thus, under selective reaction conditions, enzymatic degradation, reinforcement, recycling, and upcycling of PCL- $\gamma$ CD-PU were successfully performed for more sustainable PU resources (Figure 1). Impressively, different catalyzed reaction behaviors of PCL- $\gamma$ CD-PU were achieved by one enzyme, highlighting the power of enzymes in addressing polymeric materials and the significance of polymer structure and reaction condition design.

## RESULTS AND DISCUSSION

### Polymer design and preparation

PCL-PU with three kinds of polymer structures named PCL- $\gamma$ CD( $x$ )-PU (movable crosslinks), /PCL-PU (linear structure), and PCL-C( $y$ )-PU ( $N, N, N', N'$ -tetrakis(2-hydroxyethyl)ethylene-diamine) (THEED)-based covalent crosslinks) were prepared through convenient one-step polymerization ( $x$  = mol % of TAC $\gamma$ CD and  $y$  = mol % of THEED in PCL-PU, respectively). The synthetic procedure of PCL- $\gamma$ CD( $x$ )-PU is shown in Figure 2A. The mixture of TAC $\gamma$ CD-diol and PCL-diol ( $M_n$  = 3.5 kDa) was under sonication (power at 40 W and oscillation frequency at 42 kHz) at 60°C for 30 min to form the host-guest complexes, which were then reacted with hexamethylene diisocyanate (HDI) in dry  $N, N$ -dimethylformamide (DMF) catalyzed by dibutyltin diacetate (DBTDA) at 60°C under  $N_2$ . After 24 h, the reaction solution was directly precipitated into a cold solvent of dichloromethane (DCM)/MeOH to obtain the PCL- $\gamma$ CD( $x$ )-PU. Films were prepared via solvent casting in Teflon mold and then cut into dumbbell shapes used for tensile testing. For comparison, /PCL-PU (Figures 2B and S11) and PCL-C( $y$ )-PU (Figures 2C and S14) were prepared through same one-step polymerization. The prepared films of PCL-PU are similar in color and transmittance regardless of the polymer structures, as outlined in Figures 2D–2F and S23. The gel permeation chromatography (GPC) results of PCL-PU were shown in Figure S24 and Table S3.

Subsequently, the chemical structures of PCL-PU were characterized with nuclear magnetic resonance (NMR) spectroscopy and Fourier transform infrared (FTIR) spectroscopy. Compared with PCL-diol, the chemical shift of proton at 4.70–4.90 ppm and carbon at 156.81 ppm belonging to the carbamate group (–NHCOO–) in  $^1H$  NMR and  $^{13}C$  NMR, respectively (Figures S5–S10, S12, S13, and S15–S20), corresponding to the appearance of N–H stretching bands at 3,400–3,380 and 1,535–1,520  $cm^{-1}$  belonging to carbamate group in FTIR (Figure S25), indicate that PCL-PU successfully formed.<sup>41</sup> Furthermore, the movable crosslinks in PCL- $\gamma$ CD( $x$ )-PU were confirmed with 2D  $^1H$ - $^1H$  nuclear Overhauser effect spectroscopy (NOESY) NMR measurements, which showed significant correlation signals between the interior protons of TAC $\gamma$ CD and the polymer backbone (Figures S21 and S22). Notably, most ester stretching bands were free (1,720  $cm^{-1}$  in FTIR) because of the small carbamate bond proportion and flexible long PCL chain, which resulted in low contents of hydrogen bonds in PCL-PU.<sup>35</sup> Further characterizations by differential scanning calorimetry (DSC) and thermal gravimetric analysis (TGA) showed that the introduction of TAC $\gamma$ CD-based movable crosslinks has effects

## Enzymatically Sustainable Polyurethane Resources

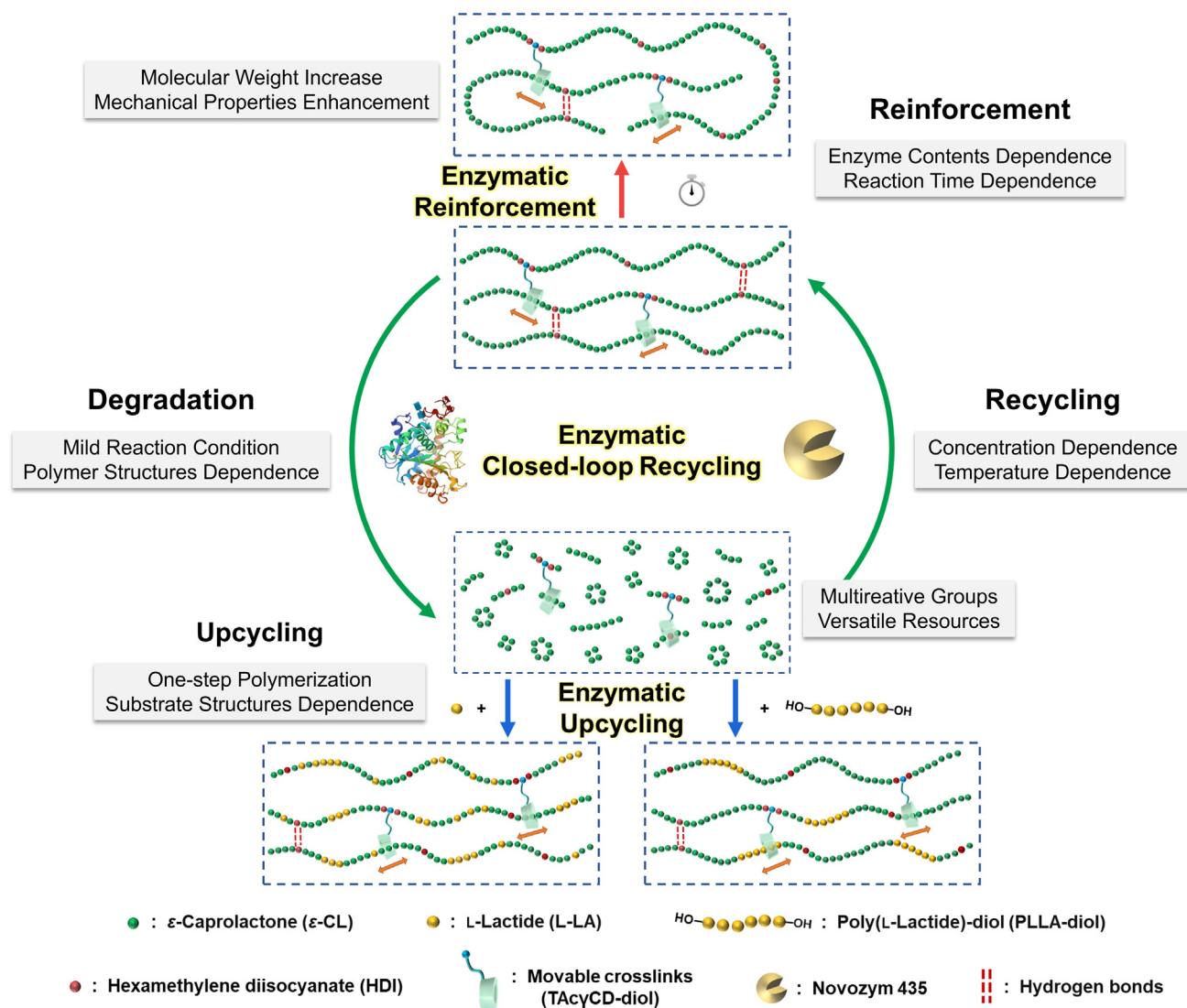


**Figure 1.** Conceptual figure showing the enzymatically sustainable resources of poly( $\epsilon$ -caprolactone)-poly(urethane) with TAC $\gamma$ CD-based movable crosslinks catalyzed by Novozym 435 as the enzyme

on the thermal properties. The glass transition temperature ( $T_g$ ) of PCL-C( $\gamma$ )-PU was similar to that of *i*-PCL-PU regardless of the THEED content, indicating that the small THEED molecule with low contents showed little effect on the thermal properties. By contrast, the  $T_g$  of PCL- $\gamma$ CD( $x$ )-PU was obviously higher than that of PCL-PU without movable crosslinks and gradually increased as the TAC $\gamma$ CD content increased, which can be attributed to the bulky structure and intrinsically high  $T_g$  of the crosslinking TAC $\gamma$ CD components that can affect the polymer structure and thermal properties (Figure S26; Table S4).<sup>54</sup> Similarly, the introduction of TAC $\gamma$ CD with high thermal stability has positive effect on PCL- $\gamma$ CD( $x$ )-PU. As a result, the decomposition temperature of PCL- $\gamma$ CD( $x$ )-PU (decomposition temperature at 5 wt % loss,  $T_{d,5\%} > 290^\circ\text{C}$ ) was higher than that of the

other polymer structures, and the complete decomposition temperature increased as the TAC $\gamma$ CD content increased (Figure S27; Table S5).

### Mechanical properties of PCL-PU

The introduction of TAC $\gamma$ CD-based movable crosslinks was expected to improve the mechanical properties of PCL-PU, which were evaluated by tensile testing at a deformation rate of 1 mm/s (Figure S28). Despite the similar physical appearances in the films, the mechanical properties were distinguished between different polymer structures (Figure 3A). According to stress-strain curves shown in Figures 3B and 3C, the mechanical properties of PCL- $\gamma$ CD( $x$ )-PU, including stiffness and ductility, were obviously better than those of *i*-PCL-PU and PCL-C( $\gamma$ )-PU. In



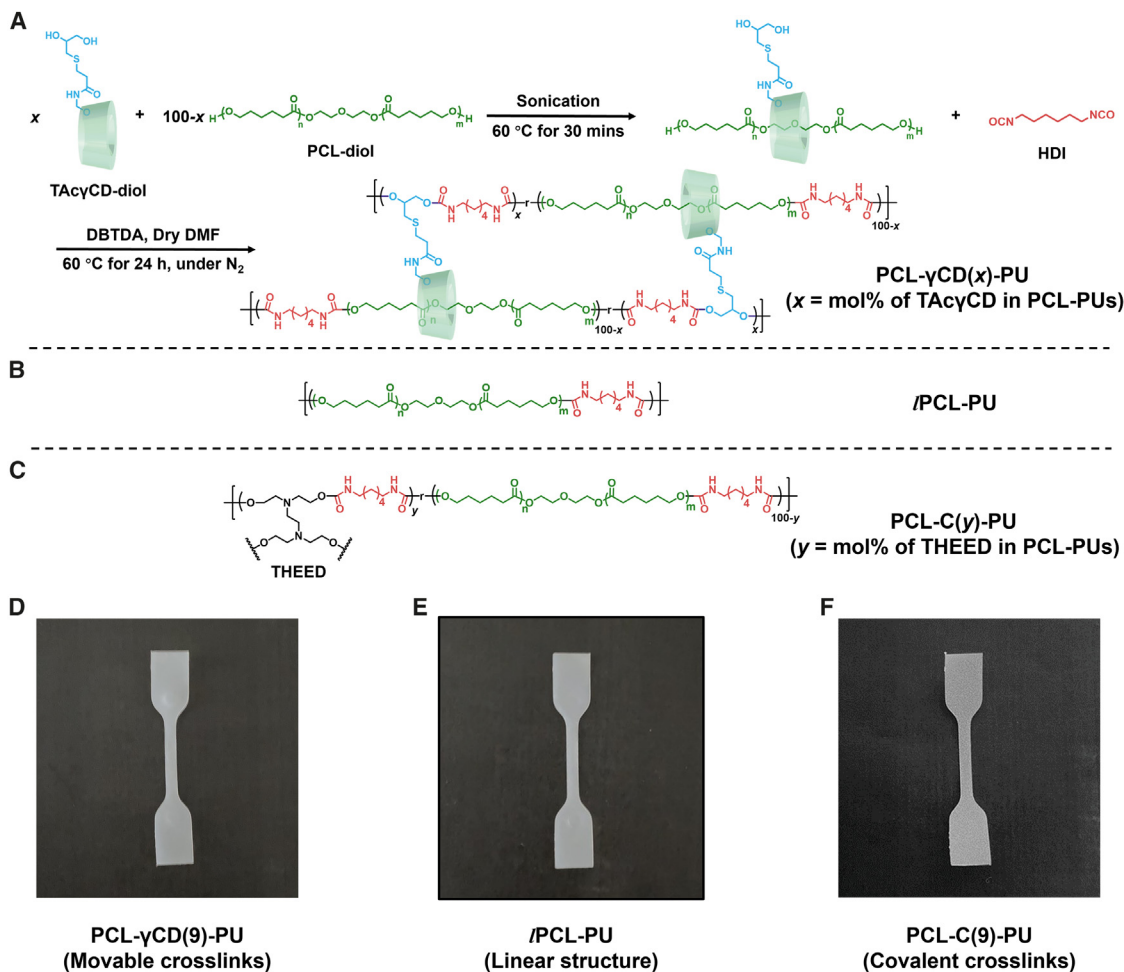


**Figure 2. The preparation of PCL-PUs**

(A) Preparation of PCL- $\gamma$ CD(x)-PU (movable crosslinks).

(B and C) Chemical structures of (B)  $\text{PCL-PU}$  (linear structure) and (C) PCL-C(y)-PU (covalent crosslinks).

(D–F) Film photographs of (D) PCL- $\gamma$ CD(9)-PU, (E)  $\text{PCL-PU}$ , and (F) PCL-C(9)-PU.

particular, the fracture stress increased from  $9.1 \pm 1.6$  MPa for  $\text{PCL-PU}$ s to  $28.4 \pm 0.6$  MPa for PCL- $\gamma$ CD(5)-PU, and the fracture strain increased from  $455 \pm 11\%$  for  $\text{PCL-PU}$ s to  $1,703 \pm 21\%$  for PCL- $\gamma$ CD(5)-PU, with only the addition of 5 mol % (3.4 wt %) TAc $\gamma$ CD. The high mechanical improvement can be attributed to the TAc $\gamma$ CD-based movable crosslinks that efficiently dispersed the local stress in PCL- $\gamma$ CD(x)-PU.<sup>47</sup> However, PCL- $\gamma$ CD(9)-PU with much higher TAc $\gamma$ CD contents (9 mol %, 6.2 wt %) performed poorly. The excessively high TAc $\gamma$ CD-based crosslinking points limited the movable ranges, thus causing stress localization and brittle network, which was similar to the negative role played by covalent crosslinks in PCL-C(y)-PU as the THEED content increased (Figure 3C).<sup>47,55</sup>

Toughness and Young's modulus (Figure 3D) were calculated from stress-strain curves, which are important indices of mechanical properties. Although covalent crosslinks greatly improved Young's modulus as the THEED content increased, the toughness of PCL-C(y)-PU reduced significantly, indicating that PCL-C(y)-PU are too brittle for practical application. Simi-

larly, the Young's modulus increased as the TAc $\gamma$ CD-based crosslinks content increased. PCL- $\gamma$ CD(9)-PU exhibited the highest Young's modulus ( $131.4 \pm 13.2$  MPa). The toughness of PCL- $\gamma$ CD(x)-PU first increased and then decreased as the TAc $\gamma$ CD content increased, and thus, PCL- $\gamma$ CD(5)-PU exhibited the highest toughness ( $250.1 \pm 10.1$  MJ m<sup>-3</sup>). Consequently, the introduction of TAc $\gamma$ CD-based movable crosslinks in PCL-PU plays a significant role in achieving comprehensive mechanical property improvements.

### Exploring the effect of polymer structures on the enzymatic reactions with 20 wt % Novozym 435

The enzymatic reaction of PCL-PU was carried out in dry toluene to investigate the potential effect of polymer structures. Given the chemical stability and low reactivity of carbamate group (urethane linkage) under mild conditions, the enzymatic reaction was focused on the ester bond belonging to the PCL segment. Among commercially available enzymes that are reactive on ester bonds, Novozym 435 is a frequently used

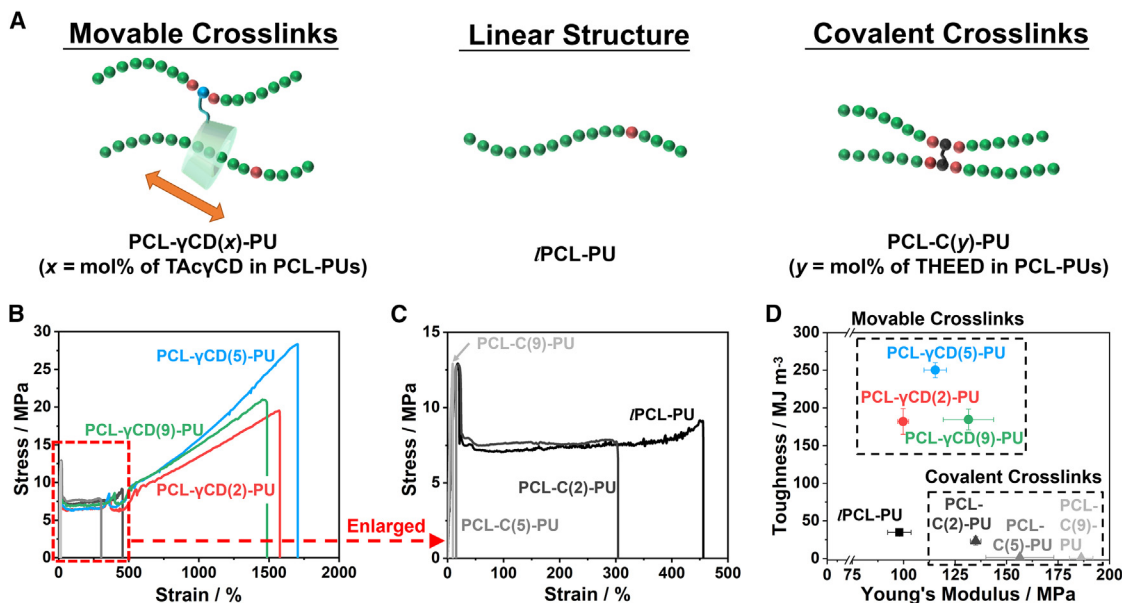


**Figure 3. The mechanical properties of PCL-PU**

(A) Schematic network of PCL- $\gamma$ CD(x)-PU, lPCL-PU, and PCL-C(y)-PU.

(B and C) Stress-strain curves of (B) PCL- $\gamma$ CD(x)-PU and (C) lPCL-PU and PCL-C(y)-PU.

(D) Relationship between toughness and Young's modulus of PCL- $\gamma$ CD(x)-PU, lPCL-PU, and PCL-C(y)-PU. Error bars represent the standard deviations based on three independent experiments.

and powerful immobilized lipase B from *Candida antarctica* (Novozym 435 contains 20–30 wt % pure lipases in a microporous acryl resin),<sup>56</sup> which can selectively catalyze a variety of aliphatic and aromatic ester-based reactions, including esterification, transesterification, polymerization, and degradation in organic solvents.<sup>26,57–66</sup> Figure 4A shows the experimental procedure with Novozym 435. The enzyme contents were determined as 20 wt % compared with the weight of PCL-PU. The PCL-PU concentration was determined to be 10 mg/mL in dry toluene. Small amounts of molecular sieves 3A were added to remove trace water. PCL-PU and degraded products are soluble in dry toluene during the reaction (Figure 4B). At each reaction time, part of the solution was collected for GPC measurement to evaluate the relationship between number-average molecular weight ( $M_n$ ) and reaction time in the enzymatic reaction.

As the reaction proceeded, the peak at high retention time (19.3–20.2 min) in the GPC diagram (Figures S30–S36) newly appeared as the signal belonging to the generated monomers (oligomers) due to the enzymatic breakage of ester bonds (Figure S29A). Although the peak intensity belonging to PCL-PU decreased, the  $M_n$  first increased and then decreased as the reaction time increased. For a short time at the beginning, since there are few generated linear monomers (oligomers) in dry toluene, the *in situ* transesterification between enzyme-PCL intermediates and other long PCL chains with terminal hydroxyl groups dominates to form longer polymer chains and regenerate the free lipases (Figure S29B), thereby increasing the  $M_n$  (Figure 4F).<sup>61–65</sup> As enzymatic reaction proceeded in dry toluene, the accumulated linear monomers (oligomers) with terminal hydroxyl groups can backbite to form the cyclic struc-

tures (intramolecular transesterification) or cleave the polymers to produce more linear monomers (oligomers), which shifted the thermodynamic reaction equilibria toward overall degradation (Figure S29C). Notably, the reaction efficiency was different depending on the polymer structures. In particular,  $M_n$  of PCL- $\gamma$ CD(9)-PU with 9 mol % TAC $\gamma$ CD decreased from 44.8 to 4.4 kDa after only 36 h (Figure 4C), demonstrating the efficient enzymatic degradation. When the TAC $\gamma$ CD content decreased to 5 and 2 mol %, a longer degradation time was observed, as PCL- $\gamma$ CD(5)-PU needed 72 h (Figure 4D) and PCL- $\gamma$ CD(2)-PU needed 120 h (Figure 4E), but the degradation was still more efficient than that of PCL-PU without TAC $\gamma$ CD-based movable crosslinks. lPCL-PU and PCL-C(y)-PU remained present in the enzymatic reaction even after 120 h (Figures 4G and S33–S36). Considering that the  $M_n$  of PCL- $\gamma$ CD(x)-PU did not simply decrease during the enzymatic reaction (Figure 4F), the degradation kinetics were studied after the polymers had reached the highest  $M_n$  ( $M_{\text{highest}}$ ) (Table S6; Figures S37 and S38). As shown in Figure S37, the enzymatic degradation of PCL- $\gamma$ CD(x)-PU tends to proceed through exponential degradation by random chain scission.<sup>24</sup> The above comparison demonstrated that the enzymatic degradation efficiency of PCL-PU increased as the TAC $\gamma$ CD content increased (Figures 4F, 4G, and S38), regardless of the pristine  $M_n$ . Moreover, the incomplete degradation was observed when higher reaction temperature (90°C) was applied (Figures S39–S46), suggesting that the enzymatic degradation activity is more suitable under mild temperature (60°C).<sup>32,66</sup>

Since the enzymatic reactions were carried out under same experimental conditions and procedure, different polymer structures are considered as the key factor contributing to

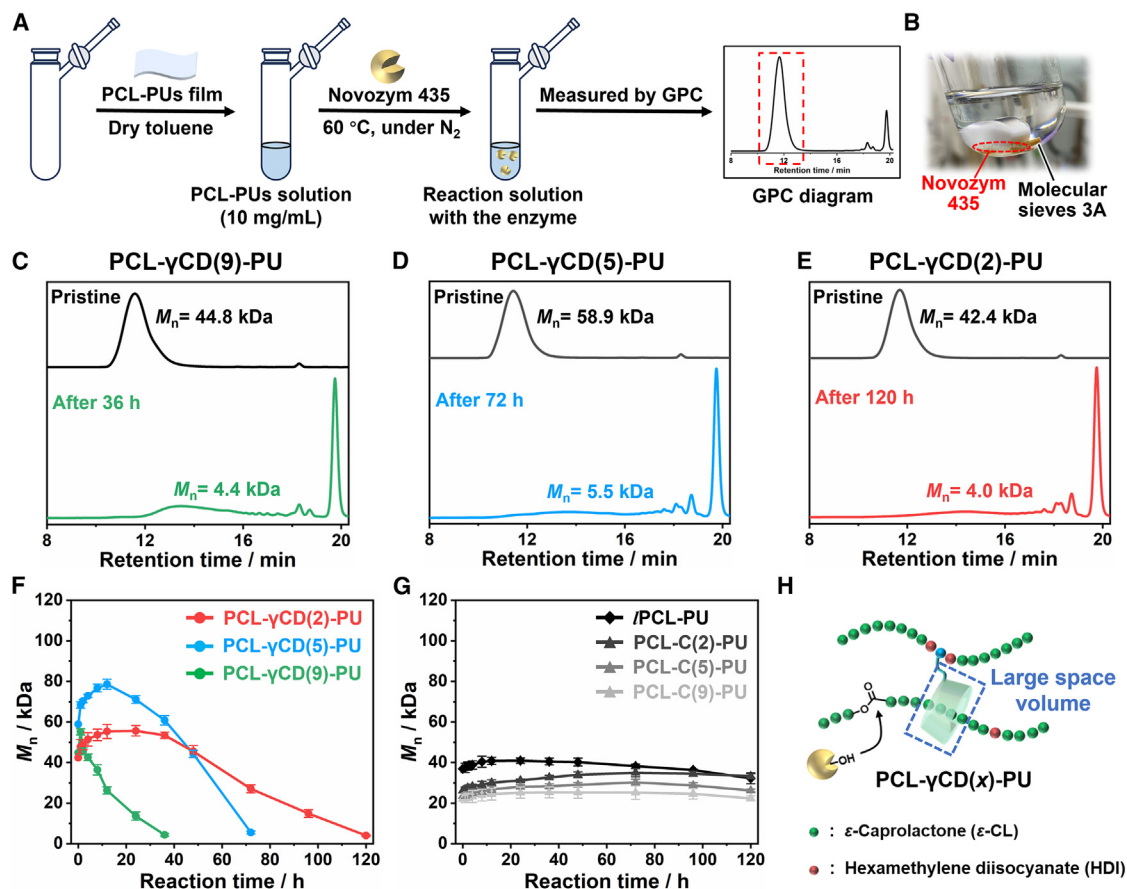


**Figure 4. The enzymatic reactions of PCL-PU with 20 wt % Novozym 435**

(A) Experimental procedure of the enzymatic reaction.

(B) Photograph of the enzymatic reaction.

(C–E) GPC diagram of pristine and degraded (C) PCL-γCD(9)-PU, (D) PCL-γCD(5)-PU, and (E) PCL-γCD(2)-PU in the enzymatic reaction with 20 wt % Novozym 435.

(F and G) The relationship between  $M_n$  and reaction time of (F) PCL-γCD(x)-PU, (G) /PCL-PU, and PCL-C(y)-PU in the enzymatic reaction with 20 wt % Novozym 435 (see Figures S30–S36). Error bars were calculated as the standard deviations.

(H) Schematic illustration of TAC<sub>γ</sub>CD with a large space volume in PCL-γCD(x)-PU.

the observed differences. Compared with the polymer structures of /PCL-PU and PCL-C(y)-PU, the significant difference in PCL-γCD(x)-PU lies in the bulky TAC<sub>γ</sub>CD as crosslinking point. Therefore, we presumed that the crosslinking TAC<sub>γ</sub>CD with a large space volume in the polymer chains introduces more free volume in the polymer network, continuously expanding the polymer network with increased TAC<sub>γ</sub>CD content (Figure 4H).<sup>67,68</sup> This also contributes to reducing the chain entanglement and local accumulation of degraded products. As a result, the access of the PU substrate (ester bond) to the enzyme was facilitated, thereby optimizing the enzymatic reaction efficiency as the TAC<sub>γ</sub>CD content increased. By contrast, with entangled and aggregated polymer networks, the access of ester sites of /PCL-PU and PCL-C(y)-PU to enzyme active site was restricted, resulting in much lower degradation efficiency. These results highlighted the advantages of CD-based topological network for designing tough and sustainable polymer resources.

### Exploring the effect of different enzyme contents on the enzymatic reactions and reinforcement strategy

Enzymatic reactions with different enzyme contents (10 and 50 wt % Novozym 435) were carried out to examine the potential effect on reaction efficiency (Figures S47–S61). Generally, all the peak intensities for PCL-PU decreased faster as the enzyme contents increased, but the variety of  $M_n$  of PCL-PU is distinguished in different polymer structures within 48 h. Because of the low reactivity of /PCL-PU and PCL-C(y)-PU with the enzyme, the  $M_n$  changed little under all enzyme contents (Figure S53). However, for PCL-γCD(x)-PU (Figures 5A–5C), the enzyme contents play a significant role in affecting and regulating the reaction behavior. First, little change in the  $M_n$  of PCL-γCD(x)-PU was observed when 10 wt % enzyme was used, indicating low reaction efficiency. When the enzyme content increased to 50 wt % enzyme, the  $M_n$  of PCL-γCD(x)-PU first increased and then decreased after a period. This result was consistent with the 20 wt % enzyme, which also showed dependence on reaction time. Additionally,



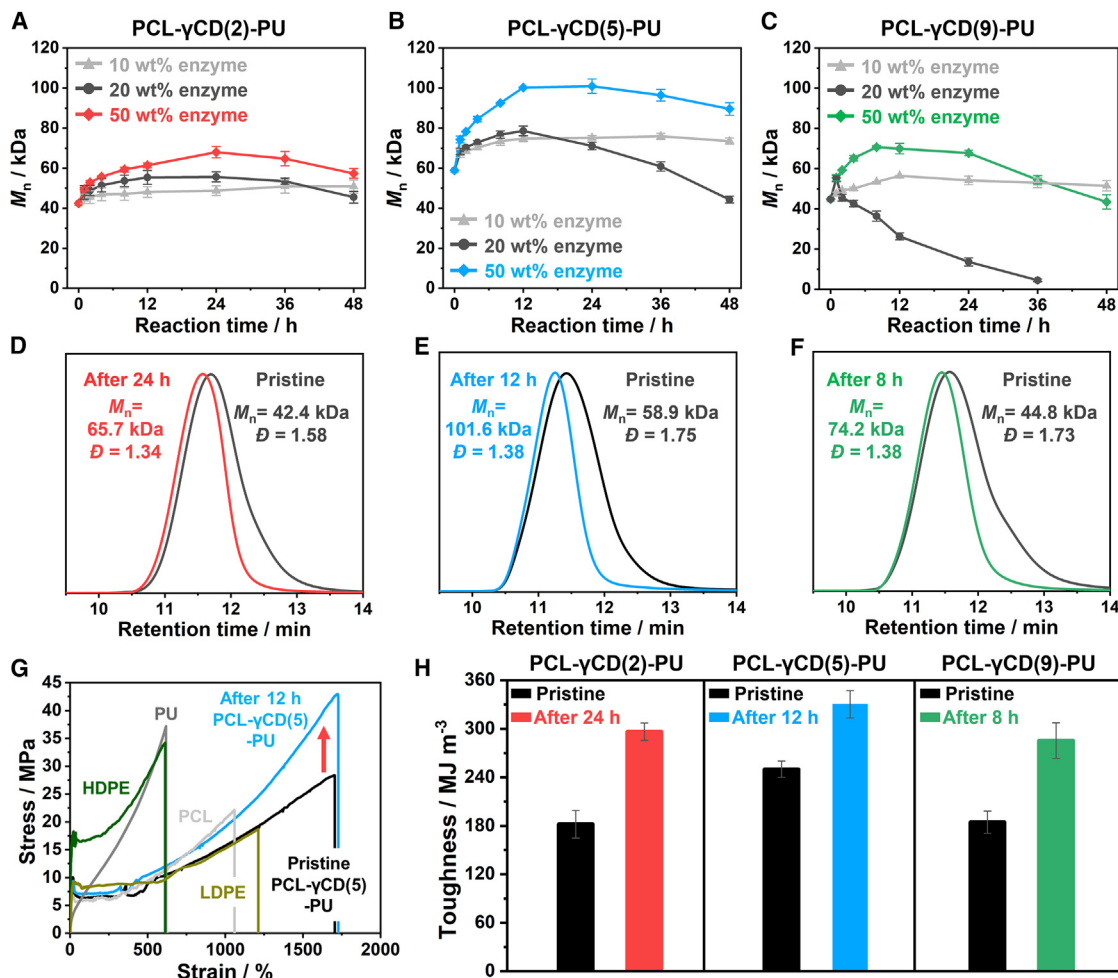


**Figure 5. The enzymatic reinforcement strategy**

(A–C) The relationship between  $M_n$  and reaction time of (A) PCL- $\gamma$ CD(2)-PU, (B) PCL- $\gamma$ CD(5)-PU, and (C) PCL- $\gamma$ CD(9)-PU in the enzymatic reactions with different contents of Novozym 435.

(D–F) GPC diagram of pristine (D) PCL- $\gamma$ CD(2)-PU, (E) PCL- $\gamma$ CD(5)-PU, (F) PCL- $\gamma$ CD(9)-PU, and after the prescribed reaction time.

(G) The stress-strain curves of commercial polycaprolactone (PCL), polyurethane (PU), low-density polyethylene (LDPE) and high-density polyethylene (HDPE), pristine PCL- $\gamma$ CD(5)-PU, and after the prescribed reaction time.

(H) The toughness of pristine PCL- $\gamma$ CD(x)-PU and after the prescribed reaction time. Error bars represent the standard deviations based on three independent experiments.

when high enzyme contents were used, the  $M_n$  of all PCL- $\gamma$ CD(x)-PU increased much more and began to decrease after a longer time. Higher contents of enzyme (50 wt %) can create more active enzyme-PCL intermediates and thereby enhance the reaction efficiency with long PCL chains with terminal hydroxyl groups to form longer polymers through enzymatic *in situ* transesterification, raising the  $M_n$  to a higher level. These polymers with higher  $M_n$  need longer time for overall degradation. Therefore, the high enzyme contents (50 wt %) were conducive to increasing  $M_n$ , while the moderate enzyme contents (20 wt %) were more suitable for degradation. The above results inspire us to design a novel reinforcement strategy of PCL- $\gamma$ CD(x)-PU that leverages the high enzyme contents (50 wt %) to highly increase the  $M_n$ , for the reason that polymers with higher  $M_n$  may perform better mechanical properties.<sup>69,70</sup>

The key point in above reinforcement strategy is to accurately control the reaction time and stop the reaction before  $M_n$  decreases. As outlined in Figures 5A–5C, 8 h were needed for PCL- $\gamma$ CD(9)-PU to obtain the highest  $M_n$ , but 12 and 24 h were needed for PCL- $\gamma$ CD(5)-PU and PCL- $\gamma$ CD(2)-PU, respectively. This observation was consistent with previous result in which the reaction efficiency was optimized as the TAc $\gamma$ CD content increased. Hence, the reaction was stopped when PCL- $\gamma$ CD(x)-PU achieved the highest  $M_n$  through enzymatic *in situ* transesterification. As the GPC results illustrated in Figures 5D–5F, the  $M_n$  of PCL- $\gamma$ CD(x)-PU successfully increased, and the dispersity ( $D$ ) of PCL- $\gamma$ CD(x)-PU decreased, indicating that longer and more uniform polymers formed. Since the monomers (oligomers) were inevitably generated throughout the enzymatic reaction (retention time between 16.0 and

20.2 min in the GPC diagram), PCL- $\gamma$ CD( $x$ )-PU with higher  $M_n$  was obtained via precipitation and filtration according to different solubility. The dissolved monomers (oligomers) were also valuable and collected as degraded products for recycling or upcycling. The  $M_n$  of all PCL- $\gamma$ CD( $x$ )-PU increased by more than 55% with yields of 60%–65%. After purification, the signals of carbamate bonds and TAC $\gamma$ CD groups were still found in NMR (Figures S63–S68) and FTIR (Figure S69), which are identical to those of the pristine polymers, confirming the presence of the movable crosslinks in PU after the enzymatic reaction.

PCL- $\gamma$ CD( $x$ )-PU with higher  $M_n$  was measured by tensile testing at a deformation rate of 1 mm/s. The obtained stress-strain curves (Figures 5G and S72) demonstrated that all the PCL- $\gamma$ CD( $x$ )-PU with higher  $M_n$  exhibited better mechanical properties. The fracture stress for all the PCL- $\gamma$ CD( $x$ )-PU increased by more than 50%. The toughness comparison (Figure 5H) further confirmed that mechanical improvements were achieved as  $M_n$  increased. The toughness increased by 63% for PCL- $\gamma$ CD(2)-PU, 32% for PCL- $\gamma$ CD(5)-PU, and 55% for PCL- $\gamma$ CD(9)-PU. Especially, PCL- $\gamma$ CD(5)-PU after enzymatic reinforcement performed better fracture stress ( $42.9 \pm 2.9$  MPa), fracture strain ( $1,724 \pm 37$  %) and toughness ( $330.4 \pm 16.9$  MJ m<sup>-3</sup>) compared with the commercial PCL, PU, low-density polyethylene (LDPE), and high-density polyethylene (HDPE), promising to be practical as commercial plastics (Figures 5G and S73). The above enzymatic *in situ* transesterification was efficient in enhancing both  $M_n$  and mechanical properties of the polymers, thus providing a novel reinforcement approach for polymeric materials.

### Exploring the enzymatic closed-loop recycling

The degraded products after enzymatic degradation can serve as building blocks for recycling or further upcycling. Prior to the recycling experiment, the products obtained from PCL- $\gamma$ CD(9)-PU degradation catalyzed by 20 wt % Novozym 435 were chosen, considering the degradation efficiency and enzyme consumption. The degraded products were then carefully characterized by NMR and electrospray ionization mass spectrometry (ESI-MS) to study the chemical structure. The signals of methylene groups adjacent to the ester oxygen at 4.06 ppm and carbonyl at 2.31 ppm mostly shifted to 4.16 and 2.37 ppm, respectively (Figures 6E and S74), consistent with the previous reports that were a mixture of cyclic and linear monomers (oligomers),<sup>57,61</sup> and the cyclic structures accounted for a large proportion. This means that under the dry reaction condition, the polymers were degraded through enzymatic transesterification, primarily forming cyclic degraded products through intramolecular transesterification. The result obtained from ESI-MS illustrated that the polymers were almost degraded into  $m/z$  lower than 1,000, containing mainly 3–5 repeating units for cyclic and linear products (Figure S76; Tables S7–S13). Notably, signals of the carbamate groups and N-H stretching bands remained present in NMR (Figures S74 and S75) and FTIR (Figure S81), demonstrating the ability of lipases to selectively attack the ester bonds.

Afterward, the degraded products at bulk and high concentration (1,000 mg/mL) were catalyzed by 20 wt % Novozym 435 at different temperatures (60°C–120°C), as lipases show

catalytic reactivity even above 100°C in organic solvent.<sup>34,71</sup> Consequently, the enzymes were powerful enough to repolymerize the degraded products into polymers, while the efficiency was distinguished (Figure 6C). The bulk polymerization, which is considered as a green approach under solvent-free conditions, was not efficient due to the increased viscosity as polymerization proceeded, thus resulting in low  $M_n$  and broad  $D$  (Figures 6C and S78). Impressively, a small addition of solvent (dry toluene) significantly optimized the reaction efficiency (Figures 6B and 6C). In addition, the efficiency ( $M_n$  increment) improved as the temperature increased, especially for the reaction at high concentration. Therefore, the optimal condition was determined to be 1,000 mg/mL at 120°C, and the  $M_n$  of the recycled polymers was 22.1 kDa. To further evaluate the enzyme renewability and reusability, the obtained polymers with  $M_n = 22.1$  kDa were degraded and repolymerized again using the same enzymes without sorting, which was achieved by simply changing the reaction concentration and temperature. As outlined in Figure 6D, the reused enzymes remain thermally stable and active, successfully catalyzing the closed-loop recycling of polymers. After purification, the signals of carbamate bonds and TAC $\gamma$ CD groups of the obtained polymers were clearly found in <sup>1</sup>H NMR (Figures 6E and S79), <sup>13</sup>C NMR (Figure S80), and FTIR (Figure S81), proving that PCL- $\gamma$ CD-PU can be conveniently closed-loop recycled despite its complex chemical structure. The biocatalyzed closed-loop recycling is powerful and has the potential to be implemented in other classes of polymer resources with diverse structures.

### Exploring the enzymatic upcycling

In addition to recycling, upcycling provides another approach to convert end-of-life polymeric materials into value-added products, which has attracted much attention these years.<sup>21,22,28,72–74</sup> In our design, the degraded products are valuable and versatile chemical resources that contain different reactive groups and pathways, thus providing an opportunity to be upcycled into value-added polymers via the convenient enzymatic reaction. To this end, commercially available monomers, L-lactide (L-LA) and  $\delta$ -valerolactone (VL), were mixed with degraded products, respectively. The enzymatic upcycling was carried out using the same conditions and procedure as in the repolymerized experiment. As outlined in Figures 7A–7C, the degraded products were almost transformed into polymers to obtain the P(CL-LLA)- $\gamma$ CD-PU and P(CL-VL)- $\gamma$ CD-PU, respectively, which were difficult to be synthesized in one step via normal chemical polymerization. After purification, the chemical structures of the upcycled copolymers were confirmed by <sup>1</sup>H NMR (Figures S83 and S84), especially the successful random copolymerization of the degraded products and L-LA into P(CL-LLA)- $\gamma$ CD-PU (Figures 7F and S83).

To further explore the different reaction pathway using same enzymatic reaction conditions and procedure, polyols with different chemical elements, the poly(L-lactide)-diol (PLLA-diols with  $M_n = 8.0$  kDa) and poly(dimethylsiloxane)-diol (PDMS-diols with  $M_n = 4.7$  kDa), were mixed with the degraded products (Figures 7D and 7E), respectively. In contrast to the upcycling strategy with L-LA cyclic monomers to achieve the

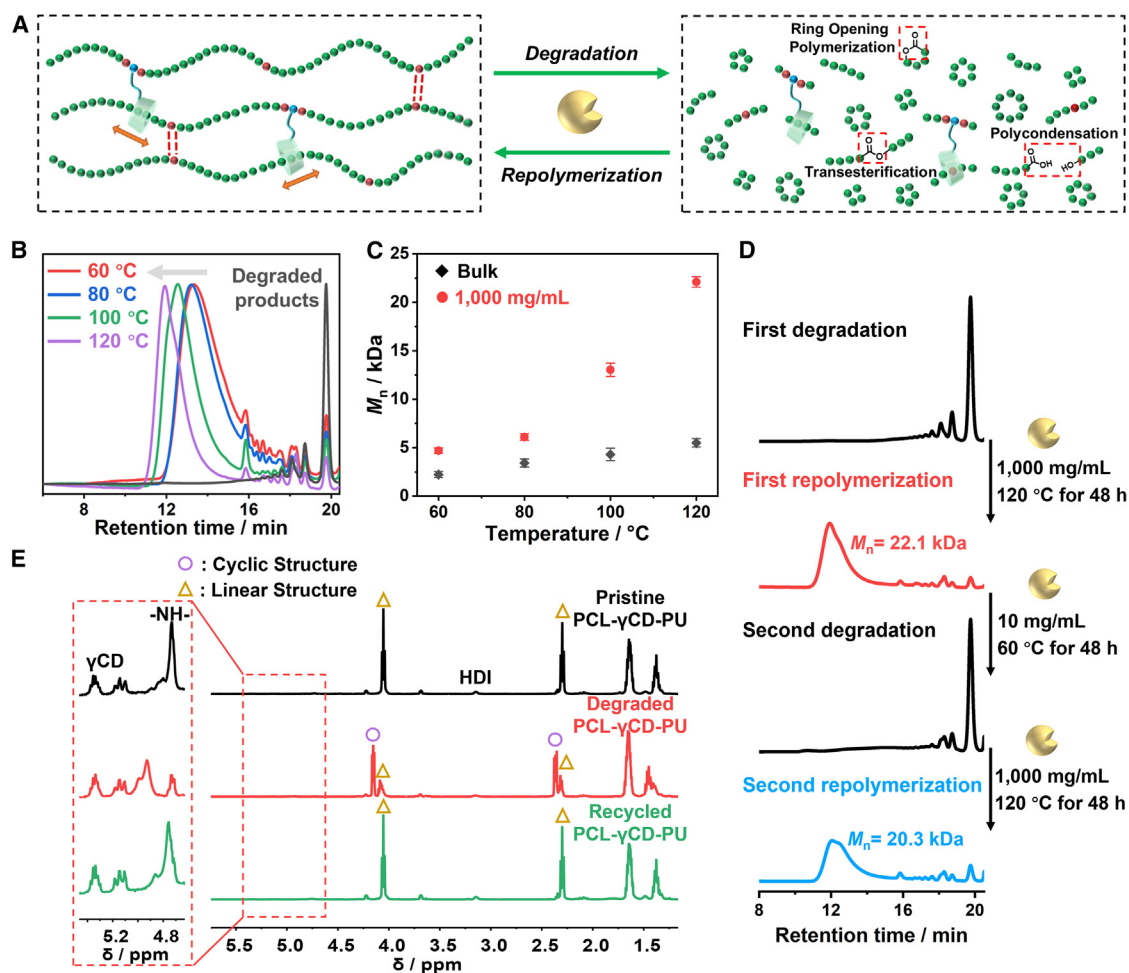


**Figure 6. The enzymatic closed-loop recycling**

(A) Schematic illustration of the enzymatic closed-loop recycling.

(B) GPC diagram of repolymerized PCL- $\gamma$ CD-PU at 1,000 mg/mL under different reaction temperatures.

(C) Relationship between  $M_n$  and reaction temperature of recycled PCL- $\gamma$ CD-PU at bulk (black) and 1,000 mg/mL (red). Error bars represent the standard deviations based on three independent experiments.

(D) Schematic illustration and GPC diagram of the repeated experiments of the enzymatic closed-loop recycling.

(E)  $^1\text{H}$  NMR of pristine (black), degraded (red), and recycled (green) PCL- $\gamma$ CD-PU.

random copolymers, the L-LA units in PLLA-diol showed no reactivity with Novozym 435 (Figure S87), and thereby the PLLA-diol with double terminal hydroxyl groups was served as a fragment to be embedded through enzymatic reaction to obtain the PCL-PLLA(a)- $\gamma$ CD-PU (a = mol % of L-LA units in PLLA-diol compared with  $\epsilon$ -CL units in degraded products) (Figure S91), as determined by  $^1\text{H}$  NMR (Figures 7F, S83, and S88–S90). The PCL-PLLA(10)- $\gamma$ CD-PU performed improved Young's modulus compared with pristine polymer (PCL- $\gamma$ CD(9)-PU) (Figure 7G), which could be attributed to the additional strongly crystalline PLLA fragments (Figure S92). Furthermore, the organic-inorganic hybrid polymers, PCL-PDMS(b)- $\gamma$ CD-PU (b = mol % of DMS units in PDMS-diol compared with  $\epsilon$ -CL units in degraded products), were successfully obtained through enzymatic upcycling of the degraded products with different ratios of PDMS-diol

(Figures S93–S96; Table S14). The hybrid feature of PCL-PDMS(b)- $\gamma$ CD-PU may show potential to be applied as polymer matrix in various areas.<sup>75,76</sup> The above results proved that the degraded products are valuable and versatile chemical resources that can react with different kinds of substrates, and the reaction pathway shows dependence on substrate structures. Based on the lipase-based enzymatic reactions with the ability to catalyze various ester-based reactions, the biocatalytic upcycling strategy is expected to be extended to diverse polymer resources, thereby producing value-added materials.

## Conclusions

We prepared topological PCL-PU with TAC $\gamma$ CD-based movable crosslinks, PCL- $\gamma$ CD-PU, that exhibited excellent mechanical properties due to effective energy dissipation. In the enzymatic reaction with Novozym 435 as the enzyme, the

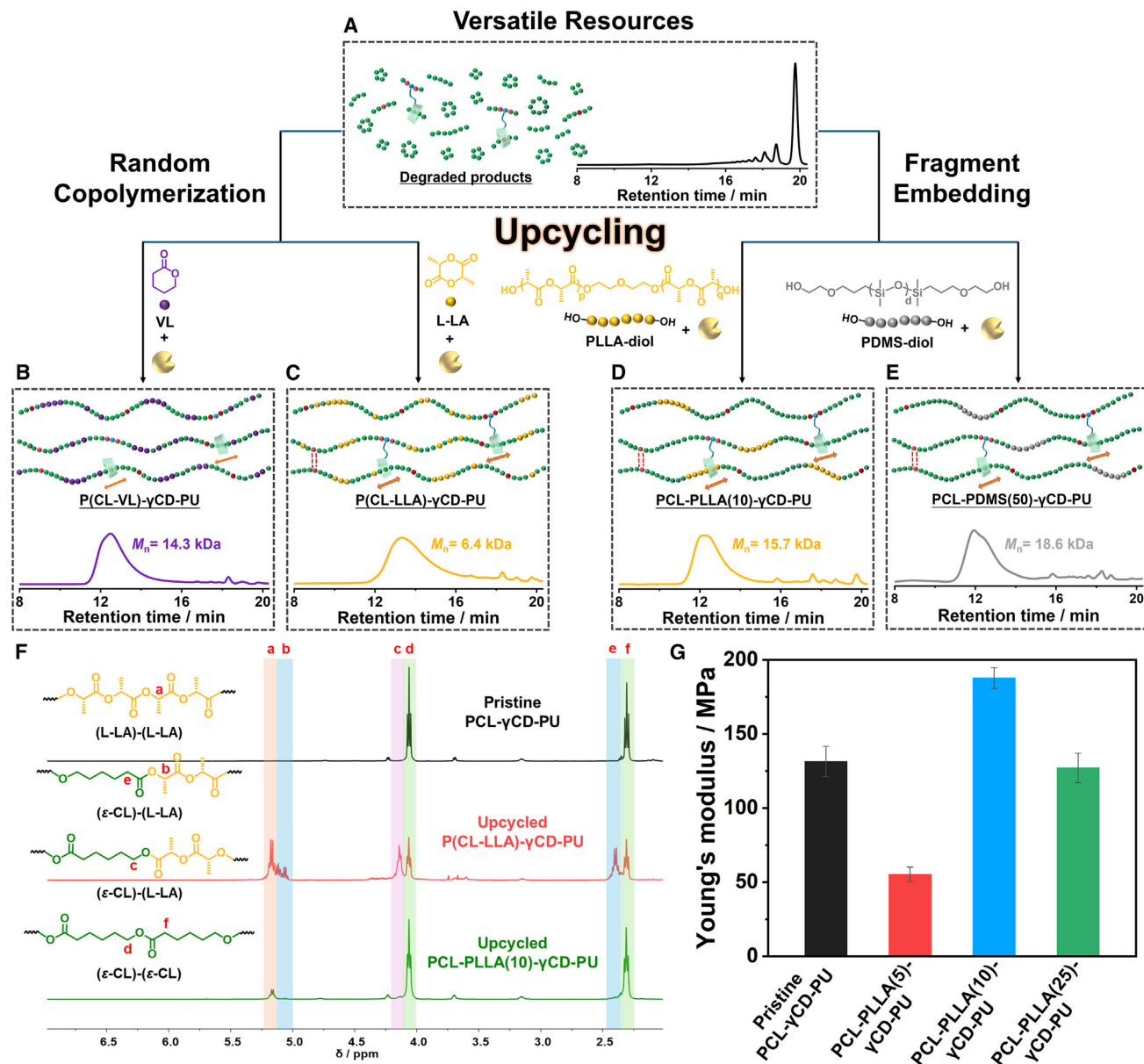


**Figure 7. The enzymatic upcycling**

(A–E) Schematic illustration and GPC diagram of (A) versatile resources (degraded products), upcycled (B) P(CL-VL)-γCD-PU, (C) P(CL-LLA)-γCD-PU, (D) PCL-PLLA(10)-γCD-PU, and (E) PCL-PDMS(50)-γCD-PU.

(F)  $^1\text{H}$  NMR of pristine PCL-γCD-PU (black), upcycled P(CL-LLA)-γCD-PU (red), and PCL-PLLA(10)-γCD-PU (green).

(G) Young's modulus of pristine PCL-γCD-PU and upcycled PCL-PLLA(a)-γCD-PU. Error bars represent the standard deviations based on three independent experiments.

obtained data demonstrated that the reaction behaviors were dependent on the polymer structures, enzyme contents, reaction time, concentration, temperature, and substrate structures in the reaction system. First, the enzymatic reaction efficiency of PCL-γCD-PU was better than that of the linear structure and covalent crosslinks, which was optimized as the TACγCD content increased due to the large space volume of TACγCD introducing more free volume in polymer network. Further investigation found that 20 wt % enzyme was suitable for

degradation, while 50 wt % enzyme was conducive to increasing the  $M_n$  of PCL-γCD-PU. Under reaction time control, a novel enzymatic reinforcement strategy for enhancing the  $M_n$  and mechanical properties of the polymers was developed. Moreover, without sorting, PCL-γCD-PU with complex chemical structure can be closed-loop recycled by switching the reaction concentration and temperature using the same enzyme, which is convenient and energy-saving. In addition to recycling, the versatile resources (degraded products) mixed with



selective substrates can be upcycled into value-added polymers via one-step enzymatic upcycling. Overall, this systematic study demonstrated the effectiveness of CD-based movable crosslinks and enzymatic reactions in enhancing the toughness of PUs and advancing their development as sustainable resources, thereby promoting their circular economy. These findings are expected to be extended to other classes of polymers, thereby contributing to a sustainable world.

## EXPERIMENTAL PROCEDURES

### Preparation of PCL-PUs

#### Preparation of PCL- $\gamma$ CD(*x*)-PU

Before reaction, all reagents (TAC $\gamma$ CD-diol and PCL-diol were mixed) were heated at 80°C under vacuum overnight to remove moisture. The mixture of TAC $\gamma$ CD-diol (*x* mol %) and PCL-diol ((100 – *x*) mol %) was under sonication at 60°C for 30 min and then dissolved in dry DMF. HDI ([NCO]/[OH] = 1.05/1) and DBTDA (0.25 wt %) dissolved in dry DMF were added to the above mixture. The reaction mixture was stirred at 60°C under N<sub>2</sub> (Figures 2A and S4). After 24 h, the reaction mixture was precipitated into cold solvent of DCM/MeOH (*v/v* = 1/4) to obtain the PCL- $\gamma$ CD(*x*)-PU. The feeding ratio is shown in Table S1.

#### Preparation of IPCL-PU

Before reaction, all reagents were heated at 80°C under vacuum overnight to remove moisture. PCL-diol (3.5 g, 1.0 mol) was dissolved in dry DMF (20 mL). Then HDI (177 mg, [NCO]/[OH] = 1.05/1) and DBTDA (9.2 mg, 0.25 wt %) dissolved in dry DMF (4.0 mL) were added. The reaction mixture was stirred at 60°C under N<sub>2</sub> (Figure S11). After 24 h, the reaction mixture was precipitated into cold solvent of DCM/MeOH (*v/v* = 1/4) to achieve the IPCL-PU.

#### Preparation of PCL-C(*y*)-PU

Before reaction, all reagents were heated at 80°C under vacuum overnight to remove moisture. THEED (*y* mol %) and PCL-diol ((100 – *y*) mol %) were mixed under sonication at 60°C for 30 min and then dissolved in dry DMF. HDI ([NCO]/[OH] = 1.05/1) and DBTDA (0.25 wt %) dissolved in dry DMF were added to the above mixture. The reaction mixture was stirred at 60°C under N<sub>2</sub> (Figure S14). After 24 h, the reaction mixture was precipitated into cold solvent of DCM/MeOH (*v/v* = 1/4) to achieve the PCL-C(*y*)-PU. The feeding ratio is shown in Table S2.

### General procedure of enzymatic reaction

PCL-PUs (100 mg) were put into Schlenk flask with dry toluene (10 mL, water content  $\leq$  20 ppm as determined by Karl Fischer titration). Novozym 435 (enzyme) with different contents (10, 20, and 50 wt % compared with the weight of PCL-PUs) and small amounts of molecular sieves 3A were added to the above solution, respectively. The reaction mixture was slightly stirred at 60°C under N<sub>2</sub>. At each reaction time, part of the solution was collected for GPC measurement.

### General procedure of enzymatic reinforcement strategy

PCL- $\gamma$ CD(*x*)-PU (800 mg) were put into Schlenk flask with dry toluene (80 mL). Novozym 435 (400 mg, 50 wt % compared with the weight of PCL- $\gamma$ CD(*x*)-PU) and molecular sieves 3A were added to the above solution. The reaction mixture was slightly stirred at 60°C under N<sub>2</sub>. The reaction was stopped at 24 h for PCL- $\gamma$ CD(2)-PU, 12 h for PCL- $\gamma$ CD(5)-PU, and 8 h for PCL- $\gamma$ CD(9)-PU, respectively. The Novozym 435 and molecular sieves 3A were removed by filtration. The reaction solution was concentrated under rotary evaporation and then precipitated into cold solvent of DCM/MeOH (*v/v* = 1/4) to obtain the PCL- $\gamma$ CD(*x*)-PU with higher *M<sub>n</sub>*. After drying, the polymers were dissolved in DCM and then poured in Teflon mold. The films were obtained by standing still at room temperature for 24 h and then at 35°C under vacuum overnight (Figures S62 and S71).

### General procedure of enzymatic degradation

PCL- $\gamma$ CD(9)-PU (1.0 g) was put into Schlenk flask with dry toluene (100 mL). Novozym 435 (200 mg, 20 wt % compared with the weight of PCL- $\gamma$ CD(9)-PU

and molecular sieves 3A were added to the above solution. The reaction mixture was slightly stirred at 60°C under N<sub>2</sub>. After 48 h, the Novozym 435 and molecular sieves 3A were removed by filtration, and then the solvent was removed under rotary evaporation. After drying, the degraded products were characterized by NMR and ESI-MS.

### General procedure of enzymatic closed-loop recycling

#### First repolymerization at 1,000 mg/mL

The products (200 mg) degraded from PCL- $\gamma$ CD(9)-PU were put into Schlenk flask with dry toluene (0.2 mL). Novozym 435 (40 mg, 20 wt % compared with the weight of degraded products) and molecular sieves 3A were added to the above solution. The reaction mixture was slightly stirred at 60°C, 80°C, 100°C, and 120°C under N<sub>2</sub>, respectively. After 48 h, part of the solution was collected for GPC measurement.

#### Second degradation at 10 mg/mL

Dry toluene (20 mL) was added to the above solution (repolymerization at 120°C), and the reaction mixture was slightly stirred at 60°C under N<sub>2</sub> to carry out the degraded experiments. After 48 h, part of the solution was collected for GPC measurement.

#### Second repolymerization at 1,000 mg/mL

The solvent was removed under vacuum. After that, dry toluene was added to keep the mixture concentration at 1,000 mg/mL. The reaction mixture was slightly stirred at 120°C under N<sub>2</sub>. After 48 h, part of the solution was collected for GPC measurement.

### General procedure of enzymatic upcycling

#### Enzymatic random copolymerization

The products (200 mg) degraded from PCL- $\gamma$ CD(9)-PU and L-LA or VL (1:1 mol % to  $\epsilon$ -CL) were put into Schlenk flask, respectively. Then dry toluene was added to keep the mixture concentration at 1,000 mg/mL. Novozym 435 (20 wt % to the total weight of reactants) and molecular sieves 3A were added to the above solution. The reaction mixture was slightly stirred at 120°C under N<sub>2</sub>. After 48 h, part of the solution was collected for GPC measurement.

#### Enzymatic fragment embedding

The products (400 mg) degraded from PCL- $\gamma$ CD(9)-PU and a mol % PLLA-diol (*a* = mol % of L-LA units in PLLA-diol compared with  $\epsilon$ -CL units in degraded products) or *b* mol % PDMS-diol (*b* = mol % of DMS units in PDMS-diol compared with  $\epsilon$ -CL units in degraded products) with different ratios were put into Schlenk flask, respectively. Then dry toluene was added to keep the mixture concentration at 1,000 mg/mL. Novozym 435 (20 wt % to the total weight of reactants) and molecular sieves 3A were added to the above solution. The reaction mixture was slightly stirred at 120°C under N<sub>2</sub>. After 48 h, part of the solution was collected for GPC measurement.

## RESOURCE AVAILABILITY

### Lead contact

Further information and requests for resources should be directed to and will be fulfilled by the lead contact, Yoshinori Takashima ([takasima@chem.sci.osaka-u.ac.jp](mailto:takasima@chem.sci.osaka-u.ac.jp)).

### Materials availability

All materials generated in this study are available from the [lead contact](#) upon reasonable request.

### Data and code availability

Detailed experimental procedures and characterization data are presented in the paper and the [supplemental information](#). Other data related to this work are available from the [lead contact](#) upon reasonable request.

## ACKNOWLEDGMENTS

This research was funded by Scientific Research on Innovative Area JP19H05714 and JP19H05721 from MEXT of Japan, the Core Research for Evolutional Science and Technology (CREST) program JPMJCR22L4 and COI-NEXT program JPMJPF2218, the Iketani Science and Technology Foundation (0341026-A and 0351026-A), the Asahi Glass Foundation, the Yazaki



Memorial Foundation for Science, the Core-to-Core Program (no. JPJSCCA20220006), the Toyota Riken Scholar Program, the International Polyurethane Technology Foundation, and the China Scholarship Council (grant no.202206150012). The authors would also like to thank the Analytical Instrument Faculty of Graduate School of Science, Osaka University, for supporting the NMR, TGA, SEM, and ESI-MS measurements and the Osaka Research Institute of Industrial Science and Technology (ORIST) for supporting the Karl Fischer titration measurement. The Novozym 435 was kindly supplied by Novozymes Japan Ltd.

## AUTHOR CONTRIBUTIONS

J.L., H.U., and Y. Takashima conceived the study. J.L. designed and conducted the experiments and characterizations, analyzed the data, and wrote the manuscript. R.I., K.Y., A.S., and J.P. contributed to the characterization support and manuscript revision. Y. Takahashi, B.K., and N.T. contributed to the financial support and cyclodextrin molecules. H.U. provided valuable suggestions for enzymatic experiments. Y. Takashima oversaw the project and contributed to the execution of the experiments and interpretation of the results.

## DECLARATION OF INTERESTS

The authors declare no competing interests.

## SUPPLEMENTAL INFORMATION

Supplemental information can be found online at <https://doi.org/10.1016/j.chempr.2024.09.026>.

Received: March 23, 2024

Revised: July 20, 2024

Accepted: September 24, 2024

Published: October 29, 2024

## REFERENCES

- Stubbins, A., Law, K.L., Muñoz, S.E., Bianchi, T.S., and Zhu, L. (2021). Plastics in the earth system. *Science* 373, 51–55. <https://doi.org/10.1126/science.abb0354>.
- Stegmann, P., Daioglou, V., Londo, M., van Vuuren, D.P., and Junginger, M. (2022). Plastic futures and their CO<sub>2</sub> emissions. *Nature* 612, 272–276. <https://doi.org/10.1038/s41586-022-05422-5>.
- Nava, V., Chandra, S., Aherne, J., Alfonso, M.B., Antão-Geraldes, A.M., Attermeyer, K., Bao, R., Bartrons, M., Berger, S.A., Biernaczyk, M., et al. (2023). Plastic debris in lakes and reservoirs. *Nature* 619, 317–322. <https://doi.org/10.1038/s41586-023-06168-4>.
- Geyer, R., Jambeck, J.R., and Law, K.L. (2017). Production, use, and fate of all plastics ever made. *Sci. Adv.* 3, e1700782. <https://doi.org/10.1126/sciadv.1700782>.
- Kwon, D. (2023). Three ways to solve the plastics pollution crisis. *Nature* 616, 234–237. <https://doi.org/10.1038/d41586-023-00975-5>.
- Coates, G.W., and Getzler, Y.D.Y.L. (2020). Chemical recycling to monomer for an ideal, circular polymer economy. *Nat. Rev. Mater.* 5, 501–516. <https://doi.org/10.1038/s41578-020-0190-4>.
- Engels, H.W., Pirkel, H.G., Albers, R., Albach, R.W., Krause, J., Hoffmann, A., Casselmann, H., and Dormish, J. (2013). Polyurethanes: Versatile materials and sustainable problem solvers for today's challenges. *Angew. Chem. Int. Ed. Engl.* 52, 9422–9441. <https://doi.org/10.1002/anie.201302766>.
- Akindoyo, J.O., Beg, M.D.H., Ghazali, S., Islam, M.R., Jeyaratnam, N., and Yuvaraj, A.R. (2016). Polyurethane types, synthesis and applications - a review. *RSC Adv.* 6, 114453–114482. <https://doi.org/10.1039/C6RA14525F>.
- Simón, D., Borreguero, A.M., de Lucas, A., and Rodríguez, J.F. (2018). Recycling of polyurethanes from laboratory to industry, a journey towards the sustainability. *Waste Manag.* 76, 147–171. <https://doi.org/10.1016/j.wasman.2018.03.041>.
- Kemona, A., and Piotrowska, M. (2020). Polyurethane recycling and disposal: Methods and prospects. *Polymers* 12, 1752. <https://doi.org/10.3390/POLYM12081752>.
- Sheppard, D.T., Jin, K., Hamachi, L.S., Dean, W., Fortman, D.J., Ellison, C.J., and Dichtel, W.R. (2020). Reprocessing postconsumer polyurethane foam using carbamate exchange catalysis and twin-screw extrusion. *ACS Cent. Sci.* 6, 921–927. <https://doi.org/10.1021/acscentsci.0c00083>.
- Woodruff, M.A., and Hutmacher, D.W. (2010). The return of a forgotten polymer - Polycaprolactone in the 21<sup>st</sup> century. *Prog. Polym. Sci.* 35, 1217–1256. <https://doi.org/10.1016/j.progpolymsci.2010.04.002>.
- Sudesh, K., Abe, H., and Doi, Y. (2000). Synthesis, structure and properties of polyhydroxyalkanoates: Biological polyesters. *Prog. Polym. Sci.* 25, 1503–1555. [https://doi.org/10.1016/S0079-6700\(00\)00035-6](https://doi.org/10.1016/S0079-6700(00)00035-6).
- Iwata, T. (2015). Biodegradable and bio-based polymers: Future prospects of eco-friendly plastics. *Angew. Chem. Int. Ed. Engl.* 54, 3210–3215. <https://doi.org/10.1002/anie.201410770>.
- Haque, F.M., Ishibashi, J.S.A., Lidston, C.A.L., Shao, H., Bates, F.S., Chang, A.B., Coates, G.W., Cramer, C.J., Dauenhauer, P.J., Dichtel, W.R., et al. (2022). Defining the macromolecules of tomorrow through synergistic sustainable polymer research. *Chem. Rev.* 122, 6322–6373. <https://doi.org/10.1021/acs.chemrev.1c00173>.
- Rosenboom, J.G., Langer, R., and Traverso, G. (2022). Bioplastics for a circular economy. *Nat. Rev. Mater.* 7, 117–137. <https://doi.org/10.1038/s41578-021-00407-8>.
- Cywar, R.M., Rorrer, N.A., Hoyt, C.B., Beckham, G.T., and Chen, E.Y.X. (2022). Bio-based polymers with performance-advantaged properties. *Nat. Rev. Mater.* 7, 83–103. <https://doi.org/10.1038/s41578-021-00363-3>.
- Neelakantan, N. (2023). Polyurethanes: Foams and thermoplastics. In *Rethinking Polyester Polyurethanes*, R.S. Pomeroy, ed. (Elsevier Inc.), pp. 179–194. <https://doi.org/10.1016/B978-0-323-99982-3.00013-4>.
- Pourahmady, N. (2023). Coatings, adhesives, and sealants from polyester polyurethanes. In *Rethinking Polyester Polyurethanes*, R.S. Pomeroy, ed. (Elsevier Inc.), pp. 195–213. <https://doi.org/10.1016/B978-0-323-99982-3.00008-0>.
- Martín, A.J., Mondelli, C., Jaydev, S.D., and Pérez-Ramírez, J. (2021). Catalytic processing of plastic waste on the rise. *Chem* 7, 1487–1533. <https://doi.org/10.1016/j.chempr.2020.12.006>.
- Ellis, L.D., Rorrer, N.A., Sullivan, K.P., Otto, M., McGeehan, J.E., Román-Leshkov, Y., Wierckx, N., and Beckham, G.T. (2021). Chemical and biological catalysis for plastics recycling and upcycling. *Nat. Catal.* 4, 539–556. <https://doi.org/10.1038/s41929-021-00648-4>.
- Kosloski-Oh, S.C., Wood, Z.A., Manjarrez, Y., De Los Rios, J.P., and Fieser, M.E. (2021). Catalytic methods for chemical recycling or upcycling of commercial polymers. *Mater. Horiz.* 8, 1084–1129. <https://doi.org/10.1039/d0mh01286f>.
- Tournier, V., Topham, C.M., Gilles, A., David, B., Folgoas, C., Moya-Leclair, E., Kamionka, E., Desrousseaux, M.L., Texier, H., Gavalda, S., et al. (2020). An engineered PET depolymerase to break down and recycle plastic bottles. *Nature* 580, 216–219. <https://doi.org/10.1038/s41586-020-2149-4>.
- DelRe, C., Jiang, Y., Kang, P., Kwon, J., Hall, A., Jayapurna, I., Ruan, Z., Ma, L., Zolkun, K., Li, T., et al. (2021). Near-complete depolymerization of polyesters with nano-dispersed enzymes. *Nature* 592, 558–563. <https://doi.org/10.1038/s41586-021-03408-3>.
- Zhu, B., Wang, D., and Wei, N. (2022). Enzyme discovery and engineering for sustainable plastic recycling. *Trends Biotechnol.* 40, 22–37. <https://doi.org/10.1016/j.tibtech.2021.02.008>.
- Shoda, S.I., Uyama, H., Kadokawa, J.I., Kimura, S., and Kobayashi, S. (2016). Enzymes as green catalysts for precision macromolecular synthesis. *Chem. Rev.* 116, 2307–2413. <https://doi.org/10.1021/acs.chemrev.5b00472>.

27. Tournier, V., Duquesne, S., Guillaumot, F., Cramail, H., Taton, D., Marty, A., and André, I. (2023). Enzymes' power for plastics degradation. *Chem. Rev.* 123, 5612–5701. <https://doi.org/10.1021/acs.chemrev.2c00644>.
28. Liu, J., He, J., Xue, R., Xu, B., Qian, X., Xin, F., Blank, L.M., Zhou, J., Wei, R., Dong, W., et al. (2021). Biodegradation and up-cycling of polyurethanes: Progress, challenges, and prospects. *Biotechnol. Adv.* 48, 107730. <https://doi.org/10.1016/j.biotechadv.2021.107730>.
29. Liu, L., Li, S., Garreau, H., and Vert, M. (2000). Selective enzymatic degradations of poly (L-lactide) and poly ( $\epsilon$ -caprolactone) blend films. *Biomacromolecules* 1, 350–359. <https://doi.org/10.1021/bm000046k>.
30. Magnin, A., Pollet, E., Perrin, R., Ullmann, C., Persillon, C., Phalip, V., and Avérous, L. (2019). Enzymatic recycling of thermoplastic polyurethanes: Synergistic effect of an esterase and an amidase and recovery of building blocks. *Waste Manag.* 85, 141–150. <https://doi.org/10.1016/j.wasman.2018.12.024>.
31. Takamoto, T., Shirasaka, H., Uyama, H., and Kobayashi, S. (2001). Lipase-catalyzed hydrolytic degradation of polyurethane in organic solvent. *Chem. Lett.* 30, 492–493. <https://doi.org/10.1246/cl.2001.492>.
32. Kobayashi, S., Uyama, H., and Takamoto, T. (2000). Lipase-catalyzed degradation of polyesters in organic solvents. A new methodology of polymer recycling using enzyme as catalyst. *Biomacromolecules* 1, 3–5. <https://doi.org/10.1021/bm990007c>.
33. Ebata, H., Toshima, K., and Matsumura, S. (2000). Lipase-catalyzed transformation of poly( $\epsilon$ -caprolactone) into cyclic dicalactone. *Biomacromolecules* 1, 511–514. <https://doi.org/10.1021/bm000059y>.
34. Soeda, Y., Toshima, K., and Matsumura, S. (2005). Synthesis and chemical recycling of novel poly(ester-urethane)s using an enzyme. *Macromol. Biosci.* 5, 277–288. <https://doi.org/10.1002/mabi.200400176>.
35. Kim, Y.D., and Kim, S.C. (1998). Effect of chemical structure on the biodegradation of polyurethanes under composting conditions. *Polym. Degrad. Stab.* 62, 343–352. [https://doi.org/10.1016/S0141-3910\(98\)00017-2](https://doi.org/10.1016/S0141-3910(98)00017-2).
36. Tang, Y.W., Labow, R.S., and Santerre, J.P. (2001). Enzyme-induced biodegradation of polycarbonate-polyurethanes: Dependence on hard-segment chemistry. *J. Biomed. Mater. Res.* 57, 597–611. [https://doi.org/10.1002/1097-4636\(20011215\)57:4<597::AID-JBM1207>3.0.CO;2-T](https://doi.org/10.1002/1097-4636(20011215)57:4<597::AID-JBM1207>3.0.CO;2-T).
37. Xie, F., Zhang, T., Bryant, P., Kurusungal, V., Colwell, J.M., and Laycock, B. (2019). Degradation and stabilization of polyurethane elastomers. *Prog. Polym. Sci.* 90, 211–268. <https://doi.org/10.1016/j.progpolymsci.2018.12.003>.
38. Raghupathi, K.R., Azagarsamy, M.A., and Thayumanavan, S. (2011). Guest-release control in enzyme-sensitive, amphiphilic-dendrimer-based nanoparticles through photochemical crosslinking. *Chemistry* 17, 11752–11760. <https://doi.org/10.1002/chem.201101066>.
39. Slor, G., and Amir, R.J. (2021). Using high molecular precision to study enzymatically induced disassembly of polymeric nanocarriers: Direct enzymatic activation or equilibrium-based degradation? *Macromolecules* 54, 1577–1588. <https://doi.org/10.1021/acs.macromol.0c02263>.
40. Wegst, U.G.K., Bai, H., Saiz, E., Tomsia, A.P., and Ritchie, R.O. (2015). Bioinspired structural materials. *Nat. Mater.* 14, 23–36. <https://doi.org/10.1038/nmat4089>.
41. Yilgör, I., Yilgör, E., and Wilkes, G.L. (2015). Critical parameters in designing segmented polyurethanes and their effect on morphology and properties: A comprehensive review. *Polymer* 58, A1–A36. <https://doi.org/10.1016/j.polymer.2014.12.014>.
42. Liu, X., and Sun, J. (2021). Polymeric materials reinforced by noncovalent aggregates of polymer chains. *Aggregate* 2, 1–17. <https://doi.org/10.1002/agt2.109>.
43. Malay, A.D., Suzuki, T., Katashima, T., Kono, N., Arakawa, K., and Nishimura, K. (2020). Spider silk self-assembly via modular liquid-liquid phase separation and nanofibrillation. *Sci. Adv.* 6, eabb6030. <https://doi.org/10.1126/sciadv.abb6030>.
44. Kim, J., Zhang, G., Shi, M., and Suo, Z. (2021). Fracture, fatigue, and friction of polymers in which entanglements greatly outnumber cross-links. *Science* 374, 212–216. <https://doi.org/10.1126/science.abg6320>.
45. Jin, C., Park, J., Shirakawa, H., Osaki, M., Ikemoto, Y., Yamaguchi, H., Takahashi, H., Ohashi, Y., Harada, A., Matsuba, G., et al. (2022). Synergetic improvement in the mechanical properties of polyurethanes with movable crosslinking and hydrogen bonds. *Soft Matter* 18, 5027–5036. <https://doi.org/10.1039/d2sm00408a>.
46. Okumura, Y., and Ito, K. (2001). The polyrotaxane gel: A topological gel by figure-of-eight cross-links. *Adv. Mater.* 13, 485–487. [https://doi.org/10.1002/1521-4095\(200104\)13:7<485::AID-ADMA485>3.0.CO;2-T](https://doi.org/10.1002/1521-4095(200104)13:7<485::AID-ADMA485>3.0.CO;2-T).
47. Ikura, R., Park, J., Osaki, M., Yamaguchi, H., Harada, A., and Takashima, Y. (2019). Supramolecular elastomers with movable cross-linkers showing high fracture energy based on stress dispersion. *Macromolecules* 52, 6953–6962. <https://doi.org/10.1021/acs.macromol.9b01198>.
48. Liu, C., Morimoto, N., Jiang, L., Kawahara, S., Noritomi, T., Yokoyama, H., Mayumi, K., and Ito, K. (2021). Tough hydrogels with rapid self-reinforcement. *Science* 372, 1078–1081. <https://doi.org/10.1126/science.aaz6694>.
49. Nakahata, M., Mori, S., Takashima, Y., Yamaguchi, H., and Harada, A. (2016). Self-healing materials formed by cross-linked polyrotaxanes with reversible bonds. *Chem* 1, 766–775. <https://doi.org/10.1016/j.chempr.2016.09.013>.
50. Du, R., Bao, T., Kong, D., Zhang, Q., and Jia, X. (2024). Cyclodextrins-based polyrotaxanes: From functional polymers to applications in electronics and energy storage materials. *ChemPlusChem* 89, e202300706. <https://doi.org/10.1002/cplu.202300706>.
51. Schmidt, B.V.K.J., and Barner-Kowollik, C. (2017). Dynamic macromolecular material design—the versatility of cyclodextrin-based host–guest chemistry. *Angew. Chem. Int. Ed. Engl.* 56, 8350–8369. <https://doi.org/10.1002/anie.201612150>.
52. Zhang, J., and Ma, P.X. (2013). Cyclodextrin-based supramolecular systems for drug delivery: Recent progress and future perspective. *Adv. Drug Deliv. Rev.* 65, 1215–1233. <https://doi.org/10.1016/j.addr.2013.05.001>.
53. Zhang, Y.M., Liu, Y.H., and Liu, Y. (2020). Cyclodextrin-based multistimuli-responsive supramolecular assemblies and their biological functions. *Adv. Mater.* 32, e1806158. <https://doi.org/10.1002/adma.201806158>.
54. Kashiwagi, Y., Urakawa, O., Zhao, S., Takashima, Y., Harada, A., and Inoue, T. (2021). Dynamics of the topological network formed by movable crosslinks: Effect of sliding motion on dielectric and viscoelastic relaxation behavior. *Macromolecules* 54, 3321–3333. <https://doi.org/10.1021/acs.macromol.0c02568>.
55. Gu, Y., Zhao, J., and Johnson, J.A. (2019). A (macro)molecular-level understanding of polymer network topology. *Trends Chem.* 1, 318–334. <https://doi.org/10.1016/j.trechm.2019.02.017>.
56. Ortiz, C., Ferreira, M.L., Barbosa, O., Dos Santos, J.C.S., Rodrigues, R.C., Berenguer-Murcia, Á., Briand, L.E., and Fernandez-Lafuente, R. (2019). Novozym 435: the “perfect” lipase immobilized biocatalyst? *Catal. Sci. Technol.* 9, 2380–2420. <https://doi.org/10.1039/C9CY00415G>.
57. Knani, D., Gutman, A.L., and Kohn, D.H. (1993). Enzymatic polyesterification in organic media. Enzyme-catalyzed synthesis of linear polyesters. I. Condensation polymerization of linear hydroxyesters. II. Ring-opening polymerization of  $\epsilon$ -caprolactone. *J. Polym. Sci. A Polym. Chem.* 31, 1221–1232. <https://doi.org/10.1002/pola.1993.080310518>.
58. Kumar, A., Dhar, K., Kanwar, S.S., and Arora, P.K. (2016). Lipase catalysis in organic solvents: Advantages and applications. *Biol. Proced. Online* 18, 2. <https://doi.org/10.1186/s12575-016-0033-2>.
59. Gagnon, C., Godin, É., Minozzi, C., Sosoe, J., Pochet, C., and Collins, S.K. (2020). Biocatalytic synthesis of planar chiral macrocycles. *Science* 367, 917–921. <https://doi.org/10.1126/science.aaz7381>.
60. Kumar, A., Khan, A., Malhotra, S., Mosurkal, R., Dhawan, A., Pandey, M.K., Singh, B.K., Kumar, R., Prasad, A.K., Sharma, S.K., et al. (2016). Synthesis of macromolecular systems via lipase catalyzed biocatalytic

- p>reactions: Applications and future perspectives.
- Chem. Soc. Rev.*
- 45**
- , 6855–6887.
- <https://doi.org/10.1039/c6cs00147e>
- .
61. Bankova, M., Kumar, A., Impallomeni, G., Ballistreri, A., and Gross, R.A. (2002). Mass-selective lipase-catalyzed poly( $\epsilon$ -caprolactone) transesterification reactions. *Macromolecules* **35**, 6858–6866. <https://doi.org/10.1021/ma0202282>.
  62. Mei, Y., Kumar, A., and Gross, R. (2003). Kinetics and mechanism of Candida antarctica lipase B catalyzed solution polymerization of  $\epsilon$ -caprolactone. *Macromolecules* **36**, 5530–5536. <https://doi.org/10.1021/ma025741u>.
  63. Johnson, P.M., Kundu, S., and Beers, K.L. (2011). Modeling enzymatic kinetic pathways for ring-opening lactone polymerization. *Biomacromolecules* **12**, 3337–3343. <https://doi.org/10.1021/bm2009312>.
  64. Kumar, A., and Gross, R.A. (2000). Candida antarctica lipase B-catalyzed transesterification: New synthetic routes to copolyesters. *J. Am. Chem. Soc.* **122**, 11767–11770. <https://doi.org/10.1021/ja002915j>.
  65. Jiang, Z., Liu, C., and Gross, R.A. (2008). Lipase-catalyzed synthesis of aliphatic poly(carbonate-co-esters). *Macromolecules* **41**, 4671–4680. <https://doi.org/10.1021/ma702868a>.
  66. Sivalingam, G., Chattopadhyay, S., and Madras, G. (2003). Enzymatic degradation of poly ( $\epsilon$ -caprolactone), poly (vinyl acetate) and their blends by lipases. *Chem. Eng. Sci.* **58**, 2911–2919. [https://doi.org/10.1016/S0009-2509\(03\)00155-6](https://doi.org/10.1016/S0009-2509(03)00155-6).
  67. Fleury, G., Brochon, C., Schlatter, G., Bonnet, G., Lapp, A., and Hadzioannou, G. (2005). Synthesis and characterization of high molecular weight polyrotaxanes: Towards the control over a wide range of threaded  $\alpha$ -cyclodextrins. *Soft Matter* **1**, 378–385. <https://doi.org/10.1039/b510331b>.
  68. Mayumi, K., Osaka, N., Endo, H., Yokoyama, H., Sakai, Y., Shibayama, M., and Ito, K. (2008). Concentration-induced conformational change in linear polymer threaded into cyclic molecules. *Macromolecules* **41**, 6480–6485. <https://doi.org/10.1021/ma801021g>.
  69. Nunes, R.W., Martin, J.R., and Johnson, J.F. (1982). Influence of molecular weight and molecular weight distribution on mechanical properties of polymers. *Polym. Eng. Sci.* **22**, 205–228. <https://doi.org/10.1002/pen.760220402>.
  70. Hester, H.G., Abel, B.A., and Coates, G.W. (2023). Ultra-high-molecular-weight poly(dioxolane): Enhancing the mechanical performance of a chemically recyclable polymer. *J. Am. Chem. Soc.* **145**, 8800–8804. <https://doi.org/10.1021/jacs.3c01901>.
  71. Kumar, A., and Gross, R.A. (2000). Candida antarctica Lipase B catalyzed polycaprolactone synthesis: Effects of organic media and temperature. *Biomacromolecules* **1**, 133–138. <https://doi.org/10.1021/bm990510p>.
  72. Korley, L.T.J., Epps, T.H., Helms, B.A., and Ryan, A.J. (2021). Toward polymer upcycling—adding value and tackling circularity. *Science* **373**, 66–69. <https://doi.org/10.1126/science.abg4503>.
  73. Zhang, M.Q., Wang, M., Sun, B., Hu, C., Xiao, D., and Ma, D. (2022). Catalytic strategies for upvaluing plastic wastes. *Chem* **8**, 2912–2923. <https://doi.org/10.1016/j.chempr.2022.08.004>.
  74. Morado, E.G., Paterson, M.L., Ivanoff, D.G., Wang, H.C., Johnson, A., Daniels, D., Rizvi, A., Sottos, N.R., and Zimmerman, S.C. (2023). End-of-life upcycling of polyurethanes using a room temperature, mechanism-based degradation. *Nat. Chem.* **15**, 569–577. <https://doi.org/10.1038/s41557-023-01151-y>.
  75. Kang, J., Son, D., Wang, G.N., Liu, Y., Lopez, J., Kim, Y., Oh, J.Y., Katsumata, T., Mun, J., Lee, Y., et al. (2018). Tough and water-insensitive self-healing elastomer for robust electronic skin. *Adv. Mater.* **30**, e1706846. <https://doi.org/10.1002/adma.201706846>.
  76. Li, S., Zhang, J., He, J., Liu, W., Wang, Y., Huang, Z., Pang, H., and Chen, Y. (2023). Functional PDMS elastomers: Bulk composites, surface engineering, and precision fabrication. *Adv. Sci. (Weinh)* **10**, e2304506. <https://doi.org/10.1002/advs.202304506>.